Investigation of Cutting Temperatures Distribution in Machining Heat Treated Medium Carbon Steel on a Lathe

[1]A.G.F. Alabi, [1]T.K. Ajiboye and [2]H.D. Olusegun
[1]Department of Mechanical Engineering, Faculty of Engineering, University of Ilorin, Ilorin, Nigeria
[2]Federal University of Technology, Minna, Nigeria

Abstract: This study was carried out to on medium carbon steel subjected to various form of heat treatment operations by assessing the temperature distribution during the machining process. The model of oblique band heat source, moving in the direction of cutting in an infinite medium with an appropriate image heat source was used in this investigation. The model analysis was carried out separately on both the chip, the tool and the work material to numerically determined the temperature distribution during machining process using Finite Element Method with nodal grids. Johnson-Cook Model was used to determine the work materials flow stress upon which the material properties were determined. Stress/strain tests were conducted on the specimens to determine the materials' constant parameters which were used as the input parameters to the modeling equation written in Visual Basic 6.0. The optimum shear angle of 20° was used for the machining process and the frictional characteristics were also determined. The temperature along the shear plane AB was determined with reference to coordinate axis within the tool, workpiece and the chip using the model. The results which compare favourably with other results from literatures, provide basis for the design of machining variables for optimum and quality machined products which can also be applied in the computer programming of NC machine for precision machining.

Key words: Machining, cutting tool, heat treatment, normalized, annealed, tempered, hardened, simulated, profile

INTRODUCTION

The heat generated during machining or turning constitutes a major problem in the manufacturing industry. It is a source of cost expenditure and also constitute hazard to health, especially when coolants are used. Heat generation during the machining process was so important that it was one of the foremost topics investigated. It had earlier been observed that heat generation was responsible for the wear of the cutting tool hence, an empirical relationship between the cutting speed, tool temperature and tool life was developed (Taylor and Quinney, 1934). As a result of these findings, a more heat resistant known as High Speed Steel (HSS) was developed for both high speed and very high temperature machining. An analytical investigations of the temperature generated in machining processes were also developed (Rosenthal, 1946; Hahn, 1951; Trigger and Chao, 1951; Loewen and Shaw, 1954). Following these studies, there had been many analytical, mechanical and numerical models which simulated, the metal cutting processes. Most especially, numerical models are highly important in predicting chip formation,

computing the cutting forces, analyzing strain and strain rate, determining the temperature distribution and stresses on the cutting edge (Ozel and Zeren, 2004).

The numerical models enable the prediction of the tool life as tool wear is accurately monitored. The models analyse temperature during machining, its effect as it generates flow stress, strain and strain rate and how it causes surface asperity on the workpiece. The asperity determines the quality of the workpiece surface finish. Another important parameter considered by the models is the effect of friction. Friction between the workpiece, the cutting tool and the chip plays a significant role in the simulation of the cutting forces, stresses and temperature distribution (Karpat et al., 2005). The model of metal cutting which uses the finite element concept for calculating the temperature fields as proposed by Tay et al. (1990) was applied in this study. The investigation was carried out on the medium carbon steel specimens subjected to various form of heat treatment processes of hardening, normalizing, tempering and annealing in the temperature range of 350-850°C. The materials' properties determined from the stress strain curve was used as input parameters to an Oxley (1989)

Corresponding Author: A.G.F. Alabi, Department of Mechanical Engineering, Faculty of Engineering, University of Ilorin, Ilorin, Nigeria

type constitutive model which was developed and programmed in visual basic to determine the machining temperature distribution of the workpiece, tool and chip.

MATERIALS AND METHODS

Test specimens' preparation: A medium carbon steel with carbon content of 0.30% carbon as determined by X-ray Diffraction Technique is used in this study. Standard heat treatment procedures were adopted to heat treat the medium carbon steel (Totten, 2007). Five different samples were prepared for each test. The 1st 5 specimens were not heat-treated and were kept as untreated sample. The next batches of five samples were place in a furnace at a temperature of 850°C for a period of 3 h for the microstructure of the specimens to completely transformed. They were removed from the furnace and immediately quenched to maintain the hardened structure. The batch to be tempered after heated to 850°C were later heated to about 350°C and then allowed to cool in still air so that, the samples became softer. The batch to be normalized were heated to 850°C and then allowed to cool outside the furnace in still air. A homogenous structure of ferrite and pearlite were formed. The annealed specimens were heated in the furnace at 850°C for 3 h. The furnace was turned off and the specimen allowed to cool in the furnace while they were contained inside a cast iron box with a mixture of cast iron borings, charcoal, lime and fine sand to disallow decarburization of the specimen.

Theoretical analysis: The Finite Difference Method is one of the most popular tools when considering the analysis of temperature distribution in machining processes. Consider a classical orthogonal cutting process for the continuous two dimensional chip formation case as shown in Fig. 1. The shearing is assumed to occur on the shear plane with friction at the rake face acting on the tool-chip interface over the contact length, l. It is assumed that the total workdone in machining is converted to heat, Q. The heat generating regions are also assumed to be at the shear zone and rake face.

The application of the cutting tool at the point of action is equivalent to the application of a source of energy. The heat losses at the side surface of the chip and at the tool flank and rake face other than at the tool-chip interface are considered to be negligible.

The temperatures at the back face of the tool wedge and through a cross-section of the chip, some distance from the cutting region are assumed to be constant. It is assumed that the tool and chip achieve steady state and quasi-steady state conditions, respectively. There are two
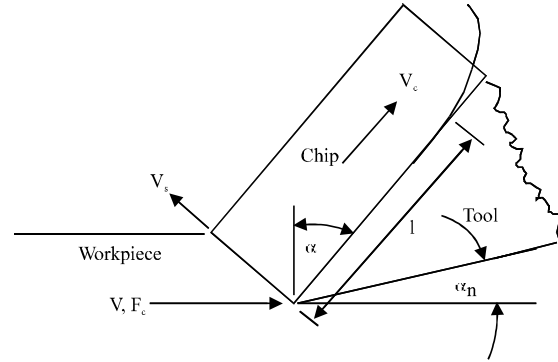

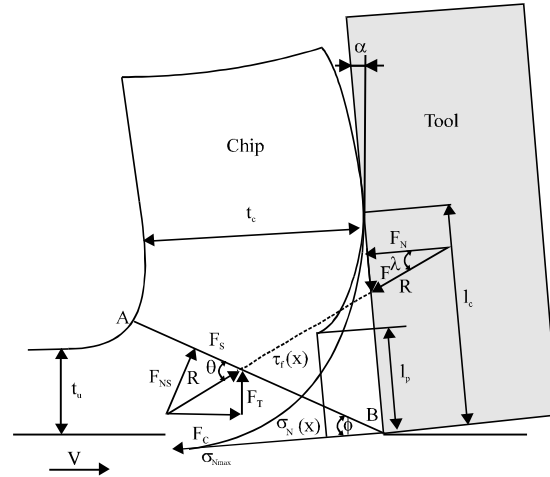Fig. 1: Continuous chip formation in orthogonal cutting process

Fig. 2: Forces acting on the shear plane and the tool with resultant stress distribution on the tool rake face (Karpat *et al.*, 2005)

important zones that give rise to the total heat, Q_T, generated during machining. They are the shear zones which generate heat given as Q_s and the heat produced on the rake face, Q_f.

It is assumed that Q_f is uniformly distributed over the contact area and that no frictional heat is transferred to the workpiece (Ceretti *et al.*, 1996). The final temperature distribution of the chip and tool system is obtained by using finite difference analysis with nodal grids and boundary conditions (Ng *et al.*, 1999). From Fig. 2 and 3, the total heat generated per unit time, Q_T is given in:

$$Q_T = Q_s + Q_f \tag{1}$$

$$Q_s = F_s V_s = \frac{\left(\tau w t_u V Cos\lambda_n\right)}{\left\{Sin\phi Cos\left(\phi-\alpha\right)\right\}} \tag{2}$$
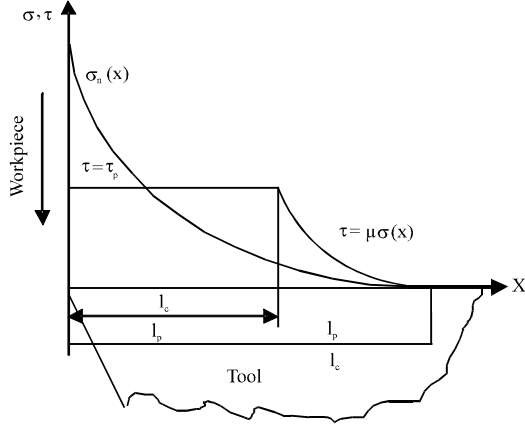
Fig. 3: Normal and frictional stress distributions on the tool rake face

$$Q_f = FV_c = \frac{\left(\tau w\, t_u\, V\mathrm{Sin}\,\lambda_n\right)}{\left\{\mathrm{Cos}\left(\phi+\lambda_n-\alpha\right)\mathrm{Cos}\left(\phi-\alpha\right)\right\}} \qquad (3)$$

$$Q_T = F_p V = \frac{\left\{\tau w\, t_u\, V\mathrm{Cos}\left(\lambda_n-\alpha\right)\right\}}{\mathrm{Sin}\,\phi\,\mathrm{Cos}\left(\phi+\lambda_n-\alpha\right)} \qquad (4)$$

The rise in the average bulk temperature of the chip due to shearing (T_s) can be found from one of the convectional shear zone thermal analysis given in (Karpat *et al.*, 2005):

$$T_s = \frac{\left(\left(1-B_1\right)Q_s\right)}{\rho\, c\, w\, t_u\, V} \qquad (5)$$

and:

$$B_1 = \frac{1}{\left[1+0.753\left(\dfrac{R_T}{\varepsilon}\right)^{\frac{1}{2}}\right]} \qquad (6)$$

Where:
F_s = Shear force
F_c = Cutting force
F = Frictional resistance of the tool acting on the chip
V_s = The velocity of the chip relative to the workpiece
V_c = The velocity of chip relative to the tool
τ = Shear stress
w = Width of cut
V = The resultant cutting speed
λ_n = Friction angle
ϕ = Shear angle
α = Normal rake angle
B = The proportion of Q_s entering the workpiece
R_T = The thermal number
ε = The plastic strain of the material of the workpiece

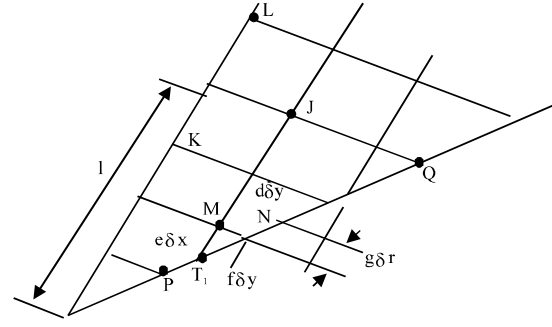$$R_T = \frac{t_u V}{\alpha} = \text{Thermal number} \qquad (7)$$

Fig. 4: Nodal points in the tool

$$\varepsilon = \mathrm{Cot}\,\phi + \tan\left(\phi-\alpha\right) \qquad (8)$$

When the chip is considered as a body in quasi-static thermal equilibrium with a moving heat source and the tool as a body in steady state thermal equilibrium with a stationary heat source, it is possible to find the final temperature in the chip and tool. By using the Cartesian Coordinate System and applying it to the Fig. 4, the generated heat conduction equations for the chip and tool are given as:

$$dvk\left[\frac{\partial^2 T}{\partial x^2}+\frac{\partial^2 T}{\partial y^2}+\frac{\partial^2 T}{\partial z^2}\right]+q$$
$$= dv\rho c\,\frac{\partial T}{\partial t_u} = dv\rho cv\,\frac{\partial T}{c\,\partial x} \qquad (9)$$

$$dvk\left[\frac{\partial^2 T}{\partial x^2}+\frac{\partial^2 T}{\partial y^2}+\frac{\partial^2 T}{\partial z^2}\right]+q = dv\rho c\,\frac{\partial T}{\partial t_u}=0 \qquad (10)$$

Where:
k = Thermal conductivity
c = Specific heat capacity
T = The average bulk temperature rise of the chip due to shearing

In finite difference form, Eq. 9 and 10 become for the chip:

$$A+q = \delta v\rho c\left[\frac{T\left(x+\delta x,\, y,\, z\right)-T\left(x-\delta x,\, y,\, z\right)}{2\delta x}\right] \qquad (11)$$

For the tool:

$$A+q = 0 \qquad (12)$$

Where:

$$A = \delta x\delta y\delta z\, k\left[\begin{array}{c}\dfrac{T\left(x+\delta x,\, y,\, z\right)+T\left(x-\delta x,\, y,\, z\right)-2T\left(x,\, y,\, z\right)}{\delta x^2}+ \\[2mm] \dfrac{T\left(x,\, y+\delta y,\, z\right)+T\left(x,\, y-\delta y,\, z\right)-2T\left(x,\, y,\, z\right)}{\delta x^2}+ \\[2mm] \dfrac{T\left(x,\, y,\, z+\delta z\right)+T\left(x,\, y,\, z-\delta z\right)-2T\left(x,\, y,\, z\right)}{\delta x^2}\end{array}\right]$$
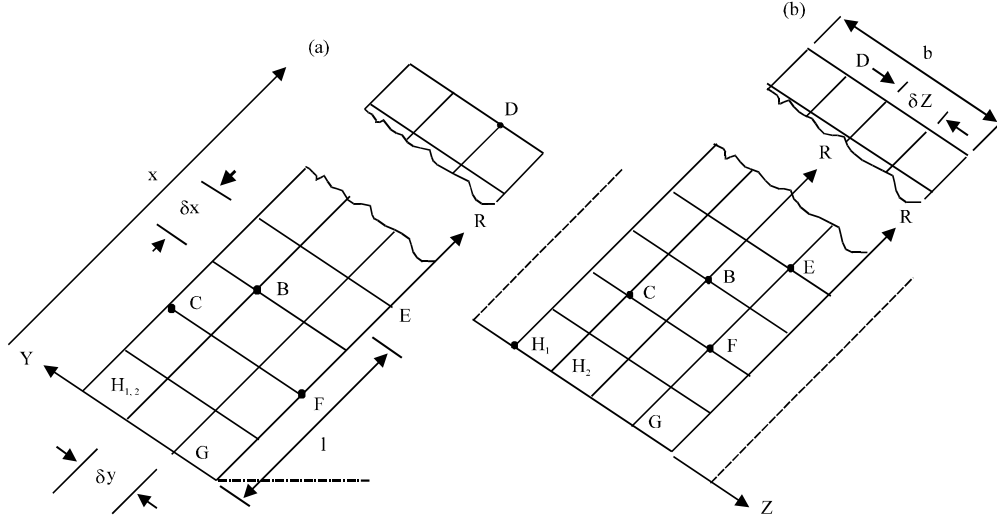$$(13)$$

Fig. 5: Nodal points inside chips

If both the chip and tool are considered, the cutting edge and common rake face plane are used to select the x and y axes as shown in Fig. 5a. The heat generated at the nodes inside the chip, Fig. 5b for example, CDEFG is assumed to be zero since, heat will only be transferred by friction and shearing. By the concept of mirror imagining at positions C and D, Fig. 5a and b, we have:

At C:

$$T\left(x,\, y+\delta y,\, z\right) = T\left(x,\, y-\delta y,\, z\right) \tag{14}$$

At D:

$$T\left(x+\delta x,\, y,\, z\right) = T\left(x-\delta x,\, y,\, z\right) \tag{15}$$

The values of Eq. 14 and 15 are used in Eq. 13. The tool is shown by Fig. 4. For internal nodes like J, q = 0. At point on the boundary such as K and L, the principles of mirror imaging is again applied. From Fig. 5, the situations differ for the nodes at the edge and those inside the grid. To develop the finite difference equations from first principles, the following steps were followed. At M, the finite difference equation is:

$$A_1 = 0 \tag{16}$$

$$A_1 = k\frac{(1+e)(1+b)\delta x \delta y \delta z}{4} = \left[2\left(\frac{eT\theta\left(x+\delta x,\, y,\, z\right)+T\left(x-e\delta x,\, y,\, z\right)-(1+e)T\left(x,\, y,\, z\right)}{e(1+e)\delta x^2}\right)+ \right.$$
$$\left. 2\left(\frac{T\left(x,\, y+d\delta y,\, z\right)+dT\left(x,\, y-\delta y,\, z\right)-(1+d)T\left(x,\, y,\, z\right)}{d(1+d)\delta y^2}\right)+\frac{T\left(x,\, y,\, z+\delta z\right)+T\left(x,\, y,\, z-\delta z\right)-2T\left(x,\, y,\, z\right)}{\delta z^2} \right] \tag{17}$$

and at N:

$$A_2 = 0 \tag{18}$$

where:

$$A_2 = \delta v k \left[\frac{T\left(x,\, y,\, z+\delta z\right)+T\left(x,\, y,\, z-\delta z\right)-2T\left(x,\, y,\, z\right)}{\delta z^2} + \frac{2}{d\delta y e \delta x}\left\{T_1 - T\left(x,\, y-d\delta y,\, z\right)-x^2\, T\left(x,\, y,\, z\right)- \right.\right.$$
$$\left.\left. \frac{(e+g)\left(f\delta y-g\delta x x\right)\delta x\, T\left(x,\, y-d\delta y,\, z\right)}{g\delta x^2\left(g+e\right)-f\delta y^2\left(f+d\right)} \right\} \right] \tag{19}$$

$$T_1 = \theta(x - T\delta x, y - d\delta y, z)$$

where, $x = \tan\alpha$ and d-g are fractions of regular nodal spacings on Fig. 4. It is important to note that the Cartesian finite grid is ideal for the chips but the analysis is more complete when considering the wedge tool because of the extra equations needed for the flank face. For the flank face, the equation for a one dimensional heat flow is given as:

$$\frac{\partial^2 T}{\partial y^2} = \frac{R_T}{t_u}\frac{\partial T}{\partial x} \tag{20}$$

When only temperature rise at the heat source is considered the temperature rise at point I on Fig. 6 caused by the entire moving band heat source is given as:

$$T_I = \frac{q_{pl}}{2\pi\lambda}\int_{-1}^{+1}e^{-VR\,Cos\left(\frac{\beta-\phi}{2a}\right)}K_0\left(\frac{V(X-1_i)}{2a}\right)dl_i \tag{21}$$

Where:
T_I = Temperature rise at point 1
q_{pl} = Heat liberation intensity
V = Resultant cutting speed
R = The distance between the moving line heat source and the point I
β = Angle between R and X-axis
a = Thermal diffusivity
ϕ = Shearing angle
K_0 = Zero order Bessel function which determines the location of the nodal points
1_i = The instantaneous point of interest on the shear plane AB
λ = The thermal conductivity

Modeling of temperature distribution in the chip: The general heat flow (Eq. 20) can now be modeled for the primary shear zone and tool-chip interface (Ozel and Karpat, 2005). According to the general solution of Eq. 21, the temperature rise at any point on the chip due to primary heat source can be found by Eq. 21 with the heat liberation intensity q_{pl}, now replaced by shear heat intensity, q_{shear} as a result of cutting and with the coordinate system shown in Fig. 6:

$$T_{shear}(X, Z) = \frac{q_{shear}}{2\pi\lambda_c}\int_{1_i=0}^{L_{AB}}e^{-(U)\frac{V_c}{2a_c}}\times\left\{K_0\left[\frac{V_c}{2a_c}\sqrt{(U)^2+(U')^2}\right]\right\}dl_i +$$

$$\frac{q_{shear}}{2\pi\lambda_c}\int_{1_i=0}^{L_{AB}}e^{-(U)\frac{V_c}{2a_c}}\left\{K_0\left[\frac{V_c}{2a_c}\sqrt{(U)^2+(2t_{ch}-U')^2}\right]\right\}dl_i \tag{22}$$
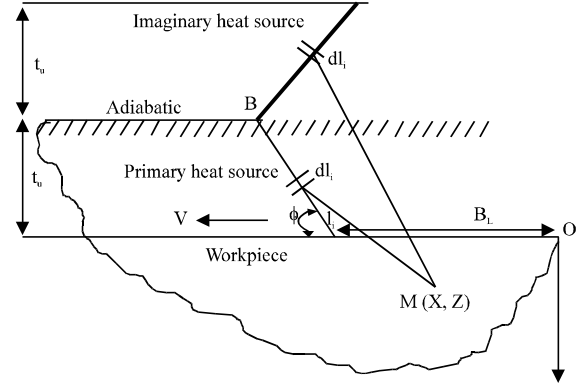

Fig. 6: Thermal modeling of primary heat source on the workpiece side adapted from Boothroyd (1963)

Where:
U = $X-l_c+l_i\,Sin\,(\phi-\alpha)$
U' = $Z-l_i\,Cos\,(\phi-\alpha)$
l_{AB} = The length of shear zone/plane
l_c = Tool-chip contact length and K_0, ϕ, α, V_c, a, λ_n are as defined previously

$$X_i = 1-l_i\,Sin(\phi-\alpha),\ Z_i = l_i\,Cos(\phi-\alpha),\ 1 = \frac{t_{ch}}{Cos(\phi-\alpha)}$$

The effect of secondary heat source along the tool-chip interface on the chip side modeled as a non-uniform moving band heat source and the temperature rise at any point in the chip due to this heat source can be calculated with Eq. 23. The tool rake face and the upper surface of the chip are considered to be adiabatic. Since, an imaginary heat source is added to the tool rake face to make this surface adiabatic, this image heat source will also have double heat intensity:

$$T_{chip-friction} = \frac{1}{\pi\lambda_c}\int_{1_i=0}^{l_c}B_i(1_i)q_f(1_i)e^{-(X-1_i)\frac{V_c}{2a_c}}\times$$
$$\left[K_0\left(R_i\frac{V_c}{2a_c}\right)+K_0\left(R_i'\frac{V_c}{2a_c}\right)\right]dl_i \tag{23}$$

Where:

$$R_i = \sqrt{(X-x)^2+Z^2}$$

and:

$$R_i' = \sqrt{(X-x)^2+(2t_{ch}-Z)^2}$$

which are the distances from heat sources, respectively. Non-uniform heat partition for the chip side and non-uniform heat intensity are denoted by $B_i(1_i)$ and $q_{pl}(1_i)$, respectively. As a result, the temperature rise at any point in the chip can be found by using Eq. 24 with the addition of room temperature T_0:

$$T_{chip} = T_{shear} + T_{chip-friction} + T_o \qquad (24)$$

The heat intensity of the primary and secondary heat sources in this study is considered uniform and can be computed as given in Eq. 25:

$$q_s = \frac{F_s V_s}{l\, w} \qquad (25)$$

Where:

F_s = Shear force on AB

q_s = Shear heat intensity, V_s, l, w are as defined previously

and:

$$q_f = \frac{F V_c}{l_c\, w} \qquad (26)$$

Where:

F = Cutting force

V_c = Chip velocity

q_f = Frictional heat intensity, l_c and w are as defined before

Modeling of temperature rise in the tool: The tool side of the secondary heat source is modeled as a non-uniform stationary rectangular heat source. In the flank surface of the tool, it is assumed that the heat lost is zero.

Also in the lower surface of the chip, there is going to be a heat generation and for effective matching of the temperature, the heating effect of the primary shear zone on the tool rake face needs to be included as given in Eq. 27:

$$T_{tool-chip}\left(X', Y', Z'\right) = \frac{1}{2\pi\lambda_t} \int_{y_i=-w/2}^{w/2} \int_{x_i=0}^{l_c} \left(1 - B_i\left(x_i'\right)\right) \times$$
$$q_{pi}\left(x_i'\right)\left(\frac{1}{R_i} + \frac{1}{R_i'}\right) dx_i dy_i \qquad (27)$$

Where:

$$R_i = \sqrt{\left(X' - x_i'\right)^2 + \left(Y' - y'\right)^2 + Z'^2}$$

$$R_i' = \sqrt{\left(X' - 2l_c + x'\right)^2 + \left(Y' - y'\right)^2 + Z'^2}$$

λ_t = Thermal conductivity of the tool material

The tool side of the rubbing heat source can be modeled as in Fig. 7 where in the tool rake face; it is assumed that the heat loss is zero. According to the coordinate system shown in Fig. 7, the temperature rise at any point on the tool due to the rubbing heat source can be written as:
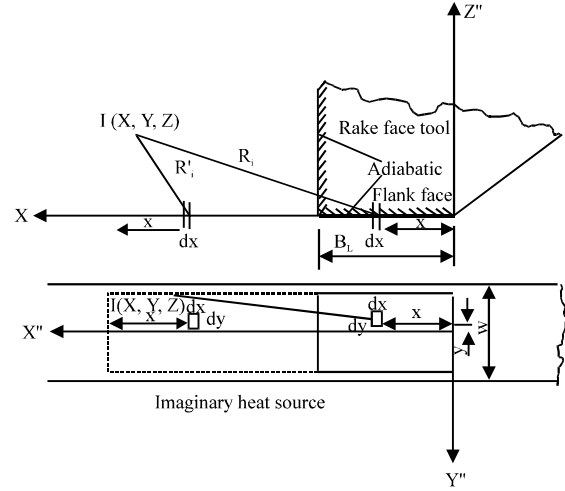

Fig. 7: Thermal modeling of rubbing heat source on the tool rake and flank faces for a blunt tool modified (Murarka *et al.*, 1981)

$$T_{M\,tool-rubbing}\left(X'', Y'', Z''\right) = \frac{1}{2\pi\lambda_t} \int_0^{B_L} \int_{-w/2}^{w/2} \left[1 - B_2\left(X''\right)\right] \times$$
$$q_{rub}\left(X''\right)\left(\frac{1}{R_i} + \frac{1}{R_i'}\right) dy'' dx'' \qquad (28)$$

Where:

$$R_i = \sqrt{\left(X'' - x''\right)^2 + \left(Y'' - y''\right)^2 + Z''^2}$$

$$R_i' = \sqrt{\left(2B_L - X'' - x''\right)^2 + \left(Y'' - y''\right)^2 + Z''^2}$$

BL is the length of blunt end of the tool and for a pointed tool, the BL = 0. The heat intensity of the rubbing heat source is modeled as non-linear by multiplying the cutting velocity and shear stress distribution. The temperature rise at any point on the tool can then be expressed as:

$$T_{tool} = T_{tool-chip} + T_{tool-rubbingi} + T_o \qquad (29)$$

In the case of a sharp tool, this rubbing heat generation will be zero hence, Eq. 29 reduces to:

$$T_{tool} = T_{tool-chip} + T_o \qquad (30)$$

Modeling of temperature rise on the workpiece: In order to model temperature rise on the workpiece, primary heat source is modeled again as an oblique moving band heat

$$T_w\left(X''', \ Z'''\right) = T_{workpiece\,shear} + T_{workpiece\,rubbing} + T_o \quad (33)$$
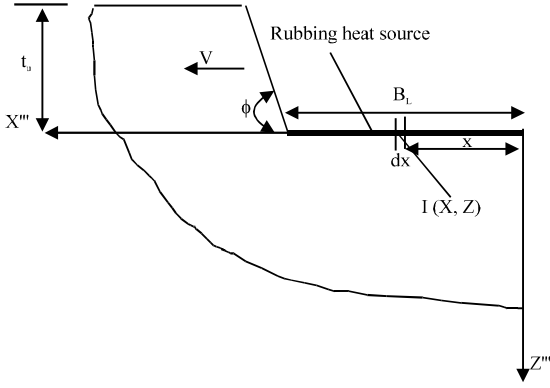

Fig. 8: Thermal modeling of rubbing heat source on the workpiece side

source which moves under the workpiece surface with cutting velocity (Guo and Yen, 2004). In the model shown in Fig. 8, it also assumed that the heat loss at the uncut workpiece surface is zero. The origin of the coordinate system in this model is assumed to be the end of flank wear width. According to the given coordinate system, the temperature rise at any point on the workpiece is given as:

$$T_{workpiece-shear}\left(X''',Z'''\right) = \frac{q_{shear}}{2\pi\lambda_c}\int_{l_i=0}^{L_{AB}} e^{\frac{\left(X'''-l_i\,Sin\phi-B_L\right)V}{2a_c}} \times$$

$$\left\{K_0\left[\frac{V}{2a_c}\sqrt{\frac{\left(B_L+l_i\,Cos\phi-X'''\right)^2+}{\left(Z'''+l_i\,Sin\phi\right)^2}}\right]+\right.$$

$$\left.K_0\left[\frac{V}{2a_c}\sqrt{\frac{\left(B_L+l_i\,Cos\phi-X'''\right)^2+}{\left(2t_u+Z'''-l_i\,Sin\phi\right)^2}}\right]\right\}dl_i$$

$$(31)$$

The rubbing heat source is modeled as a band heat source moving along the tool-workpiece surface with cutting velocity. The tool-workpiece interface is adiabatic and since the heat source does not move obliquely, the rubbing and its imaginary heat sources coincide as shown in Fig. 8. The temperature rise on the workpiece was given by Ceretti *et al.* (1996) as:

$$T_{wr}\left(X''', Z'''\right) = \frac{1}{\pi\lambda_c}\int_0^{B_L} B_2\left(X'''\right)q_{rub}\left(X'''\right)e^{\frac{\left(X'''-x'''\right)V}{2a_c}} \times$$

$$\left[K_0\left(\frac{V}{2a_c}\sqrt{\left(X'''-x\right)^2+Z'''^2}\right)\right]dx''' \quad (32)$$

Combining these, the temperature rise at any point in the workpiece is given as:

The heat partition ratios $B_1(x)$ and $B_2(x)$ indicate the energy going into the chip and workpiece, respectively and can be estimated from the following empirical equations based on a compilation of experimental data (Trigger and Chao, 1951):

$$\left.\begin{array}{l} B_1 = 0.5 - 0.35\lg\left(R_T\tan\phi\right); \ 0.04 \le R_T\tan\phi\le 10.0 \\ B_1 = 0.3 - 0.15\lg\left(R_T\tan\phi\right); \ R_T\tan\phi\ge 10.0 \end{array}\right\}$$

$$(34)$$

Where:
ϕ = Shear angle
R_T = A non-dimensional thermal number

$$R_T = \frac{\rho\,C_p\,V\,t_u}{K} \quad (35)$$

Where:
ρ = Density
C_p = Specific heat, V, t_u and K are as defined previously

If B is the fraction of the shear plane heat conducted into the workpiece i.e, the heat partition ratio of the workpiece then (1-B) is the heat partition ratio in the chip and is expressed as B_2.

RESULTS AND DISCUSSION

The high rate of material flow during machining process makes it possible for the assumption of adiabatic heat transfer which makes it possible to directly compute the temperature distribution at any point of interest located within the shear cutting regime by the coordinates axis as an exact solution due to the plastic dissipation at that point. In the low thermal conductivity material like Ti6Al4V alloy, the highest temperatures occur inside the chip while the maximum temperatures are observed on the tool rake face in machining steels (Ozel and Zeren, 2005). Using the developed model equations, the temperatures generation in both the chip, the tool and the workpiece were determined.

Based on the analysis, the temperature rise in the primary and secondary deformation zones are high and approach steady state very rapidly. As a result of the steadiness, the temperature distribution within the interface were determined as an exact value at any point of interest located within the cutting regime. The other materials' properties used with the modeling equation were determined from stress/strain tests carried out on the samples. The tool materials properties and the recommended machining speeds were shown in Table 1

Table 1: Tool materials and workpiece physical properties (Karpat *et al.*, 2005)

Characteristics	Values
Carbide tool properties	
Thermal conductivity [W/(m°C)]	46
Heat capacity [N/mm²/°C]	2.7884
Specific heat [J/kg/°C]	203
Coefficient of thermal expansion [µm/(m°C)]	4.7 at room temperature
Density [kg m⁻³]	15000
High speed steel tool properties	
Thermal conductivity [W/(m°C)]	47.8
Heat capacity [N/mm²/°C]	2.5325+0.002983°C
Specific heat [J/kg/°C]	960
Coefficient of thermal expansion [µm/(m°C)]	8.45 at room temperature
Density [kg m⁻³]	3399.5
Workpiece materials (Medium carbon steel)	
Thermal conductivity [W/(m°C)]	42.7
Heat capacity [N/mm²/°C]	3.5325+0.002983°C
Specific heat [J/kg/°C]	432.6
Coefficient of thermal expansion [µm/(m°C)]	13.05 at room temperature
Density [kg m⁻³]	7850

Table 2: Materials with their recommended cutting speed (Sharma, 2008)

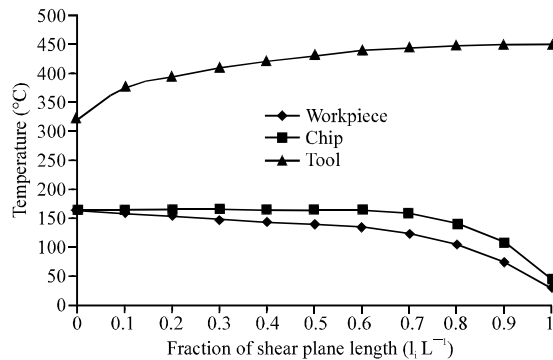| Material to be machined	Average cutting speed (m min⁻¹)
Cast iron (average)	18-30
Cast iron (hard)	12-18
Mild steel	21-25
Tool steel	12-15
Brass	45-60
Bronze	12-18

Fig. 9: Temperature distribution along the shear plane

and 2, respectively. It was observed that the temperature generation was very high at the too chip interface leaving majority of the heat with the tool immediately it separates from the tool. This was as a result of the heat generation at the secondary deformation zone and at tool-chip interface that was conducted to the cutting tool. The flank face of the tool with the workpiece is of course of low heat generation since, the model was for a sharp tool otherwise the rubbing effect will also lead to an intense heat generation in this zone. The model was also able to generates the temperature along the shear plane, AB of length, l. The shear plane AB was expressed as a ratio of the instantaneous length l_i along the shear plane, AB. The temperature profile at any point of interest along the shear plane, AB expressed as a ratio l_i/l were generated until

$l_i/l = 1$. The plot of which was shown in Fig. 9. The beauty of the model was that it gives a flexible approach to monitor the temperature profile along the shear plane, AB and to know the point of maximum or minimum temperature generation compared to the experimental which can only give the average results for a given machining condition. The temperature distribution profile for the chip, tool and the workpiece shows that the tool has the highest temperature followed by the chip and the work piece. The highest temperature of the tool was as a result of is constant contact area during machining. The chip cools faster since the contact area are not constant. The workpiece of course has the least heat distribution, since shearing only occurs at the shear plane during the machining operation.

CONCLUSION

In this study, Finite Element Modeling was utilized to simulate the temperature distribution for orthogonal cutting of medium carbon steel subjected to various form of heat treatment operations. Based on the materials' properties obtained from the stress/strain analysis, the annealed specimens gave a better machining condition within the selected machining variables as compared to tempered, normalized, hardened and the untreated. The modification of the grain structures during the heat treatment processes were observed to be responsible for these improved machining properties. The developed model gave a satisfactory result for the simulation of the chip formation and the development of the temperature distributions in the tool, chip and the workpiece. Very high and localized temperatures were observed for all the samples at the tool-chip interface due to a detailed friction model and the shearing action within the zone. The temperature profile along the shear plane AB was also analytically simulated. The temperature were however, expressed as a fraction of the instantaneous distance, l_i located by the coordinate axis in the nodal grids structure for both the tool, chip and the workpiece to obtain the temperature profile. The temperature profile obtained indicated that the tool has a higher machining temperature when machining steel materials.

NOMENCLATURE

Symbol	Meaning	Unit
Q_T	Total heat generated per unit time	W
Q_s	Heat generated along the shear zone	W
Q_f	Heat generated on the rake face	W
NC	Numerical control	
F_s	Shear force	N
F_c	Cutting forces	N
F_T	Thrust forces	N
F	Frictional force	N
V_s	Shear velocity	$m\,sec^{-1}$
V_c	Chip velocity	$m\,sec^{-1}$
τ	Shear stress	$N\,mm^{-2}$
w	Width of cut	mm
V	Resultant cutting speed	$mm\,sec^{-1}$
λ_n	Friction angle	Degree
ϕ	Shear angle	Degree
α	Normal rake angle	Degree
B	Proportion of heat generated that enter the workpiece	
R_T	Thermal number	
ε	Plastic strain of material of workpiece	
k	Thermal conductivity	$J\,m\,sec^{-1}\,{}^\circ C$
c	Specific heat capacity	
T	Average temperature rise of the chip due to shearing	$^\circ K$
q_{pl}	Heat liberation intensity of a moving plane heat source	$J\,m^{-2}\,sec$
T_1	Temperature rise at point 1	$^\circ K$
a	Thermal diffusivity	$m^2\,sec^{-1}$
K_o	Zero order Bessel function which determines the location of the nodal points	
X	The co-ordinate axis	
l_i	The instantaneous point of interest on the shear plane	
q_l	Heat liberation intensity of a moving line heat source	$J\,m^{-2}\,sec$
λ	Thermal conductivity	$J\,m\,sec^{-1}\,{}^\circ C$
R	Distance between moving line heat source and the point M	mm
β	Angle between R and X-axis	Degree
q_s	Shear heat intensity	$J\,m^{-2}\,sec$
ρ	Density	$kg\,m^{-3}$

REFERENCES

Boothroyd, G., 1963. Temperature in orthogonal metal cutting. Proc. Inst. Mechanical Eng., 177: 789-810.

Ceretti, E., P. Fallbohmer, W.T. Wu and T. Altan, 1996. Application of 2-D FEM to chip formation in Orthogonal cutting. J. Mater. Process. Technol., 59: 169-180.

Guo, Y.B. and D.W. Yen, 2004. A FEM study on mechanisms of discontinuous chip formation in hard turning. J. Mat. Process. Technol., 155-156: 1350-1356.

Hahn, R.S., 1951. On the temperature developed at the shear plane in the metal cutting process. Proceeding of 1st U.S. National Congress of Applied Mechanics, June 11-16, 1951, Chicago, IL., USA., pp: 661-666.

Karpat, Y., E. Zeren and T. Ozel, 2005. Workpiece material model based prediction for machining processes. Trans. NAMRI, 33: 413-420.

Loewen, E.G. and M.C. Shaw, 1954. On the analysis of cutting tool temperature. Trans. ASME, 26: 217-231.

Murarka, P.D., S. Hindua and G. Barrow, 1981. Influence of strain, strain-rate and temperature on the flow stress in the primary deformation zone in metal cutting. Int. J. Mach. Tool Des. Res., 21: 207-216.

Ng, E.G., D.K. Aspinwall, D. Brazil and J. Monaghan, 1999. Modeling of temperature and forces when orthogonally machining hardened steel. Int. J. Mach. Tools Manuf., 39: 885-903.

Oxley, P.L.B., 1989. Mechanics of Machining, an Analytical Approach to Assessing Machinability. Ellis Horwood Ltd., UK., ISBN: 0135686687.

Ozel, T. and E. Zeren, 2004. Determination of work material flow stress and friction for FEA of machining using Orthogonal tests. J. Mat. Proc. Technol., 154: 1019-1025.

Ozel, T. and E. Zeren, 2005. Finite element modeling of stresses induced by high speed machining with round edge cutting tools. Proceedings of the ASME International Mechanical Engineering Congress and Exposition, November 5-11, 2005, Orlando, Florida, pp: 1279-1287.

Ozel, T. and Y. Karpat, 2005. An analytical thermal modeling approach for predicting forces, stresses and temperature in machining with worn tools. Proceeding of the ASME International Mechanical Engineering Congress and Exposition, November 5-11 2005, Orlando, Florida, pp: 1-10.

Rosenthal, D., 1946. The theory of moving sources of heat and its application to metal treatments. Trans. ASME, 68: 849-866.

Sharma, P.C., 2008. A Textbook of Production Engineering. 10th Edn. S. Chand and Co. Ltd., New Delhi, India,ISBN 8121904218, 9788121904216.

Tay, O.A., M.G. Stevenson and D.G. Davis, 1990. Using the finite element method to determine temperature distribution in orthogonal machining. Proc. Institute Mechanical Eng., London, 188: 627-638.

Taylor, G.L. and H. Quinney, 1934. The latent energy remaining in a metal after cold working. Proc. R. Soc. Lond., 143: 307-326.

Totten, G.E., 2007. Heat Treatment Equipment. In: Steel Heat Treatment Equipment and Process Design, Totten, G.E. (Ed.). CRC Press, Boca Raton, FL., USA., pp: 3-192.

Trigger, K.J. and B.T. Chao, 1951. An analytical evaluation of metal cutting temperature. Trans. ASME, 73: 57-68.